EPSC Abstracts
Vol. 9, EPSC2014-482, 2014
European Planetary Science Congress 2014

Temperature and reflectance retrieval from NIR spectra

S. Erard LESIA, Observatoire de Paris/CNRS/UPMC/Univ. Paris-Diderot (stephane.erard@obspm.fr)

1. Introduction

The spectral range of NIR detectors has extended towards longer wavelengths in the recent years, and now currently encompasses the 3-5 µm region and the onset of the thermal emission of most Solar System bodies. This range contains absorptions from minerals, ices, and organic materials providing information on surface composition that is not available at shorter wavelengths. The spectral contrast is however greatly reduced because spectral features appear as absorptions in reflected light, and as peaks in emission. Study of the composition in this range therefore involves separating reflected from emitted light. Naive modeling using a constant spectral emissivity would not retrieve the original spectral contrast and precludes quantitative analyses.

The procedure used here is to fit both the spectral reflectance and the temperature in one pass. We use a basic radiance model in which reflectance and emissivity are related through a photometric function, and a single temperature is used for each pixel. However, inversions of such models are known to be numerically instable. A regularization scheme is proposed here.

2. Radiance model

The model is a simplified, atmosphereless version of the one used and described in [1]. Radiance reads:

$$L(\lambda) = r_F(i,e,\varphi)\ \frac{E_s(\lambda)}{\pi R^2} + B_\lambda\ \varepsilon(e)$$

where B_λ is the black body radiance at surface temperature T, $\frac{E_s(\lambda)}{R^2}$ is the solar irradiance at the target distance R, $r_F(\lambda)$ and $\varepsilon(\lambda)$ are the radiance factor and the directional emissivity of the surface at the same wavelength.

In a particulate medium of isotropic scatterers at thermal equilibrium, directional emissivity is related to hemispherical-directional reflectance at each wavelength by Kirchhoff's law:

$$\varepsilon(e) = 1 - r_{hd}(e) = 1 - \int_{2\pi} r_F\ d\Omega_i$$

where reflectance is integrated over incidence angles in the free half-space. This strongly depends on the phase function of the material. If the photometric function can be assumed Lambertian, which is a reasonable assumption for bright materials, Kirchhoff's law simply reads:

$$\varepsilon(e) = 1 - r_F / (\cos i)$$

This quantity does not depend on incidence in the Lambertian case, and emission is isotropic. Direct modeling can be used to simulate the rough spectrum of a bright asteroid (Fig.1).

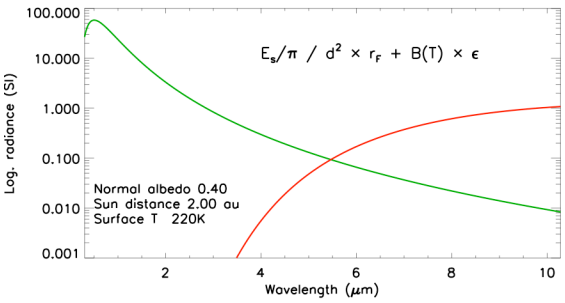

Figure 1: Simulation of asteroid Steins' radiance with the above model and a constant reflectance. From 4 to 8 µm the spectrum is a mixture of reflected and emitted light.

For darker materials, the Lommel-Seeliger model may be a better assumption. In this case, a similar, more complicated formulation of Kirchhoff's law can be derived, where emissivity is no longer isotropic.

Direct modeling has been used to retrieve the temperature of Mercury [2] and Steins [3] from NIR spectra. A similar model has been inverted to study Lutetia from VIRTIS/Rosetta observations [4, 5].

It is stressed that the spectral emissivity mentioned here is derived in the measured spectral range, therefore at short wavelengths. It may be very different from the long wavelength (~10 µm) emissivity that controls the temperature, which is typically in the 0.9-1.0 range for common minerals (against ~0.5-0.6 in Fig. 1). Such an approximation can be used to derive temperature, but can only provide spectral reflectance on the first order.

Another important problem is the influence of sub-pixel roughness and temperature variations. Roughness is often modeled using a "beaming factor" [e.g., 6], but the latter mostly stands for the photometric functions used in the present formulation. A further refinement may be to include a mix of temperatures in the field of view, although colder areas will contribute far less to the emitted radiance (~ as e^T).

3. Inversion

One may be tempted to invert the above equation directly for temperature and spectral reflectance. In practice, minimization of the Chi^2 with a simple gradient descent algorithm will find a solution quite rapidly. However, the inversion process is extremely sensitive to the noise and subject to numerical divergences, in particular near the crossover point between solar reflected light and thermal emission, which is located between 3 and 7 µm depending on the albedo, Sun distance, and thermal properties of the medium. Typically, a simple inversion results in a correct estimate of temperature but large oscillations in this range, with even negative values of the reflectance. This method is therefore not applicable if the crossover point is in the spectral range of interest.

The procedure used here consists in including a continuity constraint, i.e. to minimize the difference in retrieved reflectance between any two consecutive channels. This translates as an additional term in the Chi^2 function. The constraint prevents large oscillations to alter the reflectance spectrum, and acts as a smoothing function (similar to Wiener filtering). As opposed to Bayesian methods [5] no assumption is made on the expected spectrum, which could conceal minor absorptions.

5. Applications & prospects

This method has been applied to the inversion of VIRTIS/Rosetta observations of Lutetia (Fig. 2) and gives satisfying results with a very small failure rate (mostly related to high emergence angles). Although it provides reasonable estimates of spectral reflectance, a practical drawback is the large increase in computing time (currently ~3 min versus 10 s for a single spectrum). Once optimized, this approach will be applied to observations of 67P from the same instrument.

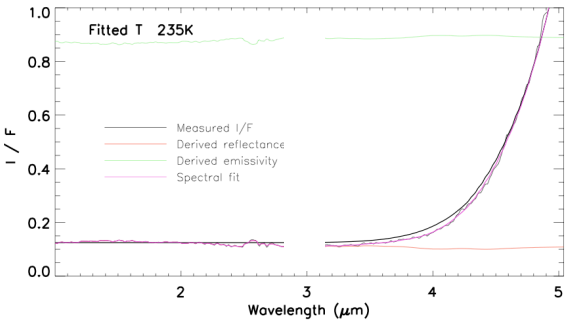

Figure 2: Temperature and reflectance determination on Lutetia (VIRTIS observations). The continuous black line is the black body I/F ratio at the retrieved temperature.

References

[1] Erard S. and Calvin W. (1997) New composite spectra of Mars, 0.4-5.7 µm. *Icarus* 130 , 449-460.

[2] Erard S., Bézard B., Doressoundiram A., Despan D. (2011) Mercury resolved spectroscopy from NTT. *Planet. Space Sci*. **49**, 1842-1852.

[3] Leyrat C., Coradini A., Erard S., Capaccioni F., Capria M. T., Drossart P., De Sanctis M.C., Tosi F., and the VIRTIS Team (2011) Thermal properties of the asteroid (2867) Steins as observed by VIRTIS/Rosetta. *Astron. & Astrophys.* **531**, A168.

[4] Coradini A., et al (2011) The Surface Composition and Temperature of Asteroid 21 Lutetia as observed by Rosetta/Virtis. *Science* **334**, 492.

[5] Keihm S., et al (2012) Interpretation of combined infrared, submillimeter, and millimeter thermal flux data obtained during the Rosetta fly-by of Asteroid (21) Lutetia. *Icarus* **221**, 395–404.

[6] Davidsson B., et al (2009) Physical properties of morphological units on Comet 9P/Tempel 1 derived from near-IR Deep Impact spectra. *Icarus* **201**, 335–357.